LA-UR- 04-7092

Approved for public release; distribution is unlimited.

Title: MONTE CARLO SIMULATION OF THE PARTICLE CHANNELS OF THE COMBINED X-RAY SENSOR AND DOSIMETER (CXD) FOR GPS BLOCK IIR AND BLOCK IIF

Author(s): Thomas E. Cayton, LANL, ISR-1

Submitted to:

Los Alamos NATIONAL LABORATORY

Form 836 (8/00)

Monte Carlo Simulation of the Particle Channels of the Combined X-Ray sensor and Dosimeter (CXD) for GPS Block IIR and Block IIF

by

Thomas E. Cayton

Abstract

Electron and proton flux response functions have been calculated for each of the 16 energetic particle channels of the CXD instrument using the Los Alamos Monte Carlo radiation transport codes. The response functions were calculated for electron and proton energies representative of those present in the space radiation environment. These response functions may be used to predict the counting rates in the CXD channels due to an incident particle spectrum. Numerical integration of an energy spectrum of incident particles with the response functions yields the counting rates in the CXD particle channels that may be compared with observed counting rates.

SENSOR DESCRIPTION : The CXD instrument[1] includes three subsystems that measure energetic particles: (1) The Low-Energy Particle (LEP) detector uses a "stack" silicon sensor (five 500-micrometer-thick silicon sensors) to measure the energy deposited by 0.14 Mev to 1.25 MeV electrons (five channels) and 6-10 MeV and >10 MeV protons (two channels). (2) The first High-energy X-ray and Particle detector (HXP1) uses a transmission mounted 300-micrometer-thick silicon"delta-E" detector element together with a CsI(Tl)/photodiode "E" element. HXP1 resolves charged particle into seven coincidence channels according to the simultaneous energy depositions in the "delta-E" and "E" elements. Six of the seven channels measure electrons (1.3 MeV to >5.8 MeV), while one measures protons (>16 MeV). (3) The second High-energy X-ray and Particle detector (HXP2) uses a CsI(Tl)/photodiode sensor element and resolves high-energy protons into two channels (10-50 MeV and >50 MeV). Particle data are reported in near-real time via the NDS Augmentation Payload (NAP) downlink and ground system; these data also are recorded in on-board memory for downloading during routine contact with the space vehicle (once per day).

The 16 CXD particle channel designations and the nominal ranges of incident energy (MeV) are as follows.

E1	0.14 - 0.23
E2	0.23 - 0.41
E3	0.41 - 0.77
E4	0.77 - 1.25
E5	1.26 - 68
E6	1.3 - 1.7

E7	1.7 - 2.2
E8	2.2 - 3.0
E9	3.0 - 4.1
E10	4.1 - 5.8
E11	>5.8
P1	6.0 - 10.
P2	10. – 50
P3	16 – 128
P4	57 - 75
P5	>75

The estimated mass and power consumption of a "dosimeter only" CXD is about 6.8 kg and about 5 W.

NUMERICAL SIMULATIONS : Flux response functions, in units of cm^2-sr/particle, for electrons and protons incident on the CXD particle sub-systems were calculated using MCNP (the Los Alamos Monte Carlo N-Particle code)[2] for the transport of electrons and secondary photons, and LAHET (the Los Alamos High-Energy Transport code)[3] for the transport of protons and secondary particles produced in high-energy nuclear interactions. Both codes us the same basic geometry package to describe complex three-dimensional geometries filled with multiple materials. These state-of-the-art radiation transport codes are part of the Los Alamos Radiation Transport Code System and are maintained by the Diagnostics and Applications Group, X-5, at Los Alamos National Laboratory.

At the time the calculations were performed, the standard codes did not permit multi-cell correlated pseudo-pulse-height tallying of the energies deposited in cells representing the active elements of coincidence detectors. The codes were therefore modified to provide a three-parameter pulse-height distribution of the energy deposited by the primary and secondary particles and photons simultaneously in three different active elements. The pulse-height distribution tally was used to calculate the electron and proton response functions which, when folded with appropriate electron and proton incident spectra, yield the channel counting rates that may be compared directly with measured data.

Geometry – Schematic drawings of the LEP and HXP1 particle subsystems used in the Monte Carlo simulations are shown in Figs. 1 and 2, respectively. Each of the subsystems is mounted in an annular sensor deck

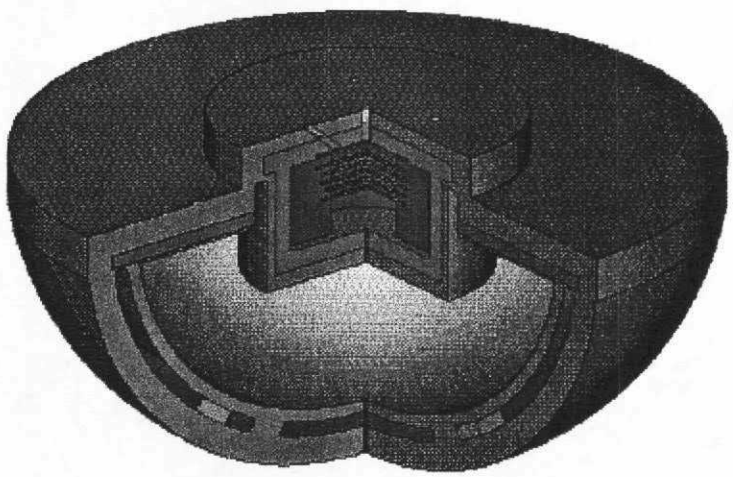

Figure 1. Simulation geometry for the LEP subassembly

and upon a hemispherical package used as a simple representation of the CXD box itself. The five spherical sections below the sensors are lumped-element masses representing the electronics modules and their covers; the lumped elements consist of mixtures ofG-10, Al, and Ta

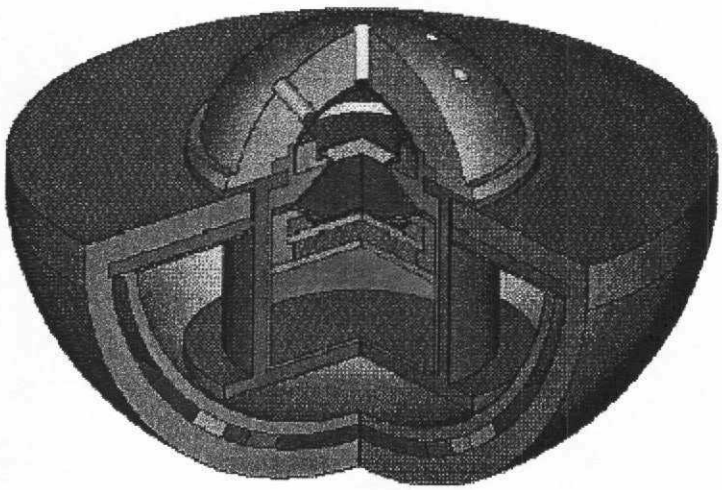

Figure 2. Simulation geometry for the HXP1 subassembly

The HXP2 subassembly resembles HXP1 except it lacks a delta-E silicon sensor, and its shield lacks collimating holes. HXP2 also uses a thicker filter within its shield.

Sources used to calculate response functions – The source used to compute detector responses was an isotropic distribution of monoenergetic particles (electrons or protons) incident on the simulation geometry either from above or from below. This enables decomposition of the total response function into separate "front-side" and "back-side" contributions. In the case of incident electrons, the front-side response itself was decomposed into two contribution corresponding to electrons impinge on the "dome" and on the "deck", respectively. To realize isotropic fluxes from above or below particles were emitted from one hemisphere of a spherical surface concentric with, but larger than, the simulation volume. The emission was uniform from each element of surface area and according to a cosine distribution relative to the unit normal of each area element (i.e., the inward-pointing radius vector).

Response functions – Pulse-height distributions were compiled for incident electrons in the energy range 0.10 to 16 MeV, and for incident protons in the range 5 to 900 MeV. All pulse heights greater than or equal to the lower deposited-energy threshold and less than the upper deposited-energy threshold of a particular channel contribute to the response of that channel. In each case, the flux response is the absolute flux per unit particle fluence delivered to the active element of the sensor and is expressed in units of cm^2-sr per incident particle.

The computed electron flux response functions for channels E1 through E11 and P3 are plotted in (Appendix A) Figs. 3 – 15. The other channels, P1, P2, P4, and P5 are totally insensitive to electrons and are not shown. In all cases red lines represent the responses arising from electrons incident on the dome shield of the detectors themselves; the blue

lines, the responses due to electrons incident on the hemispherical box; the magenta lines are responses to electrons that impinge on the annular sensor deck.

The computed proton flux response functions for channels E1 through E11 and P1 through P5 are plotted in (Appendix B) Figs. 16 – 31. The response arising from protons incident from above are show with red lines, and those arising from protons incident from below are shown with the blue lines.

Conclusion : Electron and proton flux response functions have been calculated for each of the 16 energetic particle channels of the CXD instrument using the Los Alamos Monte Carlo radiation transport codes. The response functions were calculated for electron and proton energies representative of those present in the space radiation environment. These response functions may be used to predict the counting rates in the CXD channels due to an incident particle spectrum. Numerical integration of an energy spectrum of incident particles with the response functions yields the counting rates in the CXD particle channels that may be compared with observed counting rates.

ACKNOWLEDGMENTS

The Monte Carlo simulations described herein are one part of a collaborative effort of numerical modeling by Ckuck Ingraham, Michel Tuszewski, and the author. Many of the ideas used here were stimulated by extensive discussions among the collaborators. The lumped-element masses were determined by weighted path-length averaging of the actual CXD box and was provided to the author by Chuck Ingraham. This work was performed under the auspices of the United States Department of Energy.

REFRENCES

1. The CXD Team, "The Combined X-Ray Dosimeter (CXD) on GPS Block IIR Satellites," Los Alamos National Laboratory Report LA-UR-99-2280 (1999).

2. J. F. Briesmeister, Ed., "MCNP- A General Monte Carlo Code for Neuton and Photon Transport," Los Alamos National Laboratory Report LA-7396-M, Rev. 2 (September 1986).

3. R. E. Prael and H Lichtenstein, "Users Guide to LCS: The Lahet Code System," Los Alamos National Laboratory document LA-UR-89-3014 (September 1989).

Appendix A: Electron Response Functions

(Channels E1 to E11, and P3 respond to incident electrons)

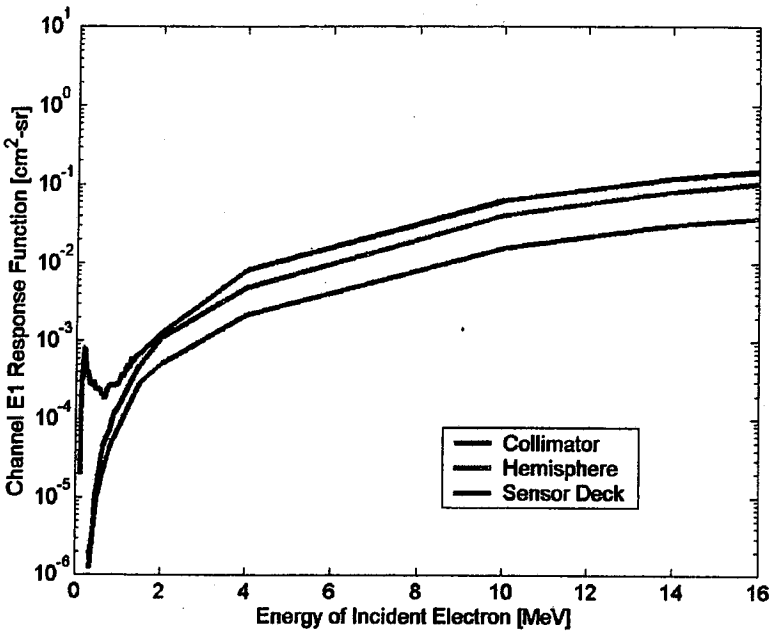

Figure 3. The numerically computed flux response of Channel E1L for an isotropic flux of electrons incident on the LEP subassembly. The red line represents the response from electrons incident on the LEP collimator plate. The blue line, the response from electrons incident on hemispherical "box". The magenta line, the response from electrons impinging on the annular "sensor deck".

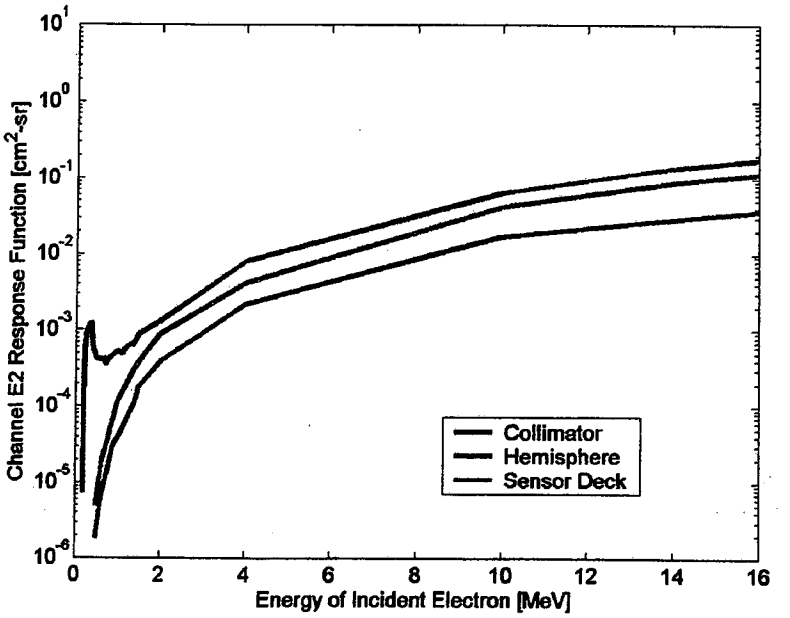

Figure 4. The same quantities as shown in Fig. 3, but for Channel E2.

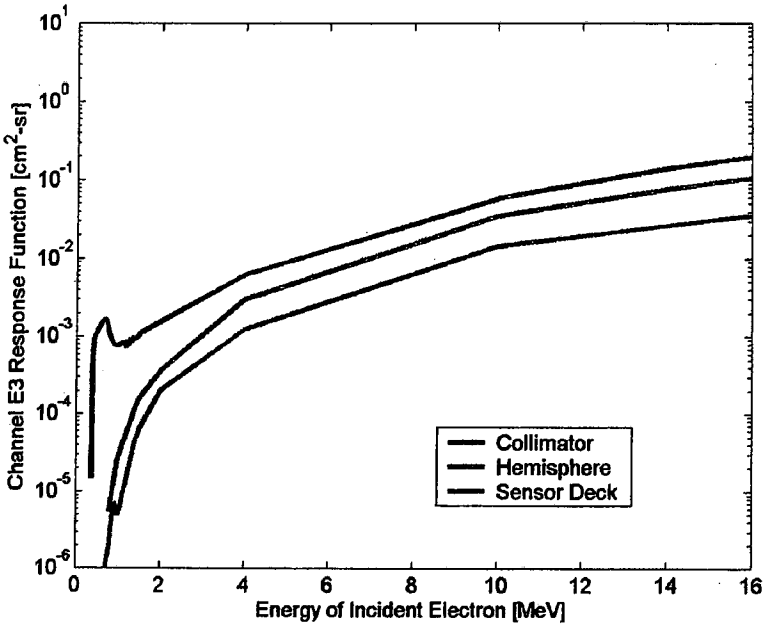

Figure 5. The same quantities as shown in Fig. 3, but for Channel E3.

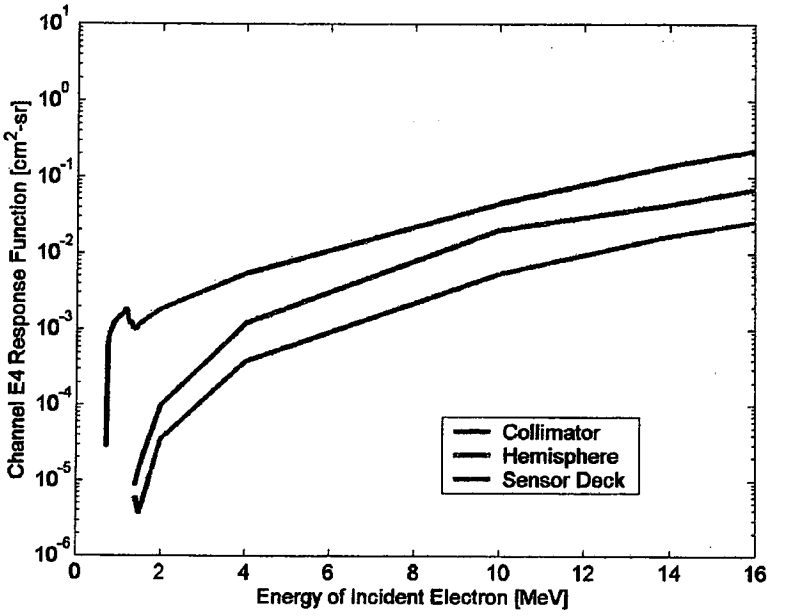

Figure 6. The same quantities as shown in Fig. 3, but for Channel E4.

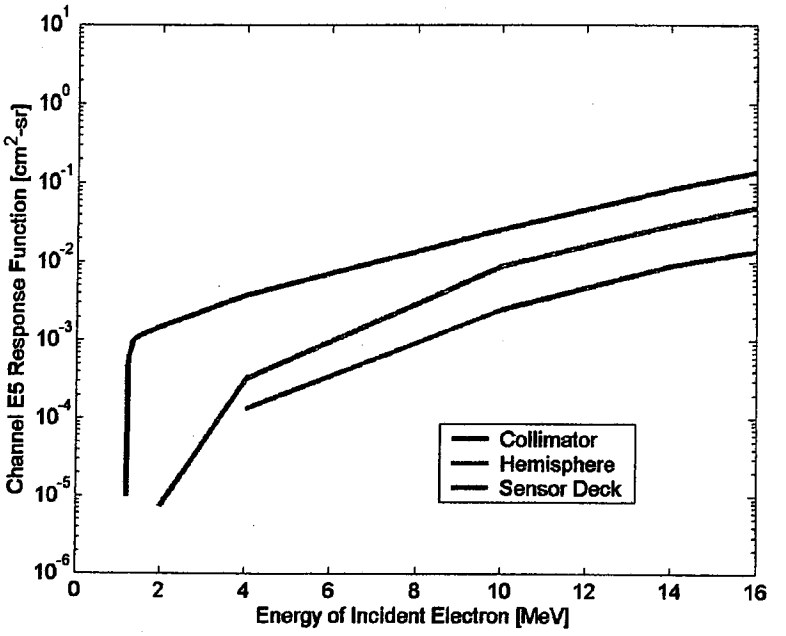

Figure 7. The same quantities as shown in Fig. 3, but for Channel E5.

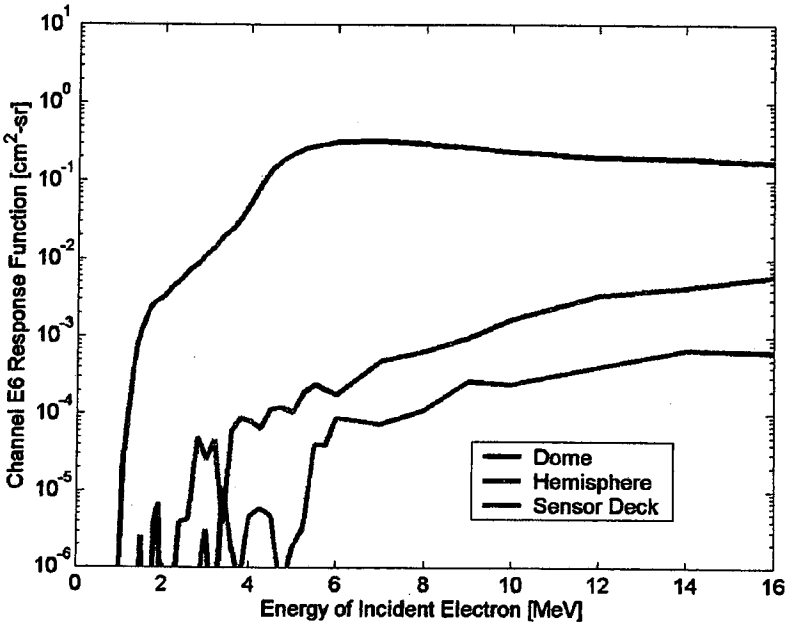

Figure 8. The numerically computed flux response of Channel E6 for an isotropic flux of electrons incident on the HXP1 subassembly. The red line represents the response from electrons incident on the HXP1 shield. The blue line, the response from electrons incident on hemispherical "box". The magenta line, the response from electrons impinging on the annular "sensor deck".

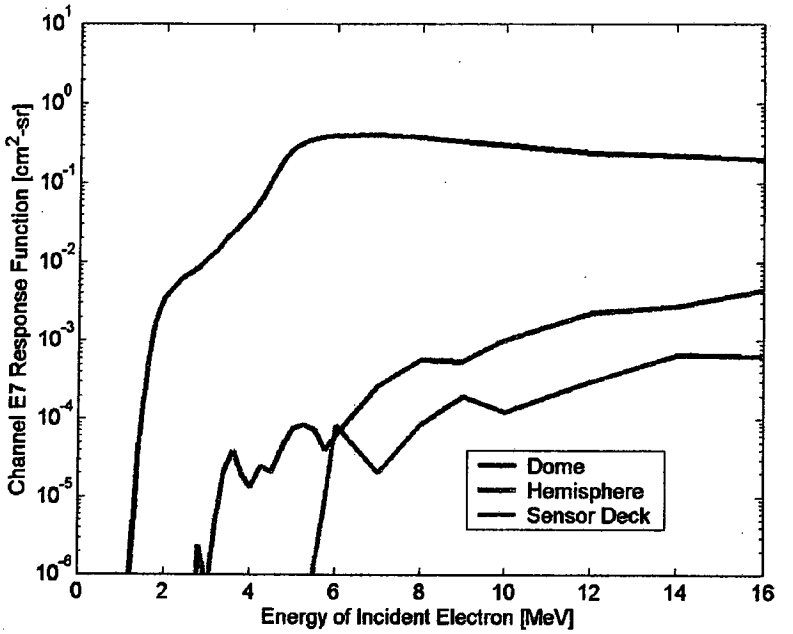

Figure 9. The same quantities as shown in Fig. 8, but for Channel E7.

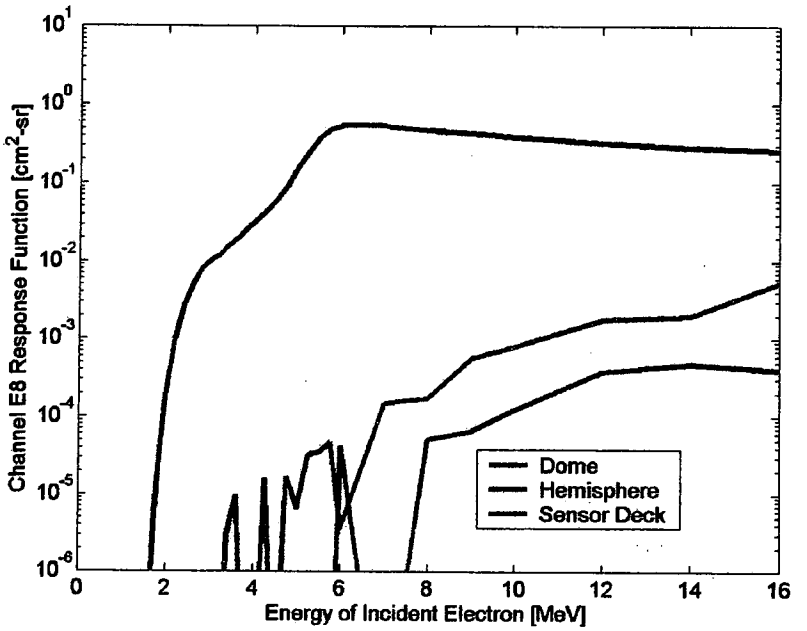

Figure 10. The same quantities as shown in Fig. 8, but for Channel E8.

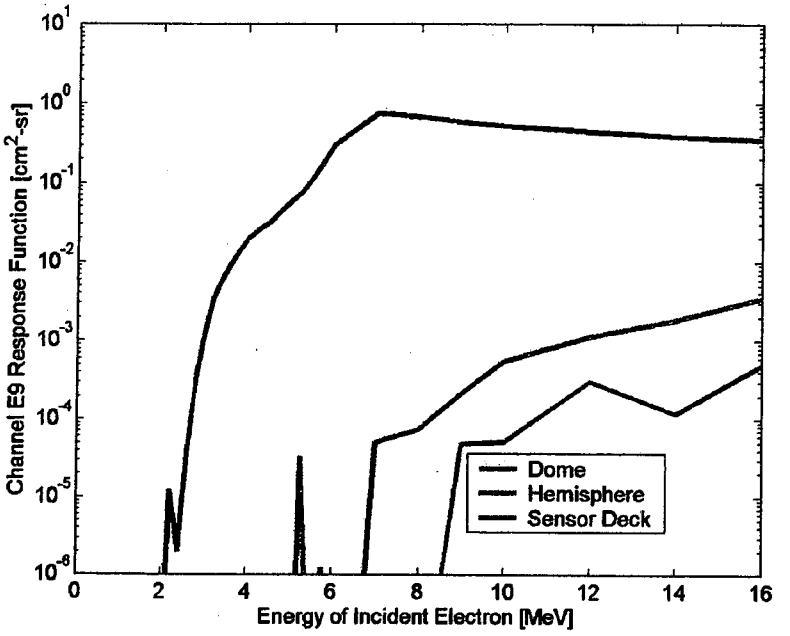

Figure 11. The same quantities as shown in Fig. 8, but for Channel E9.

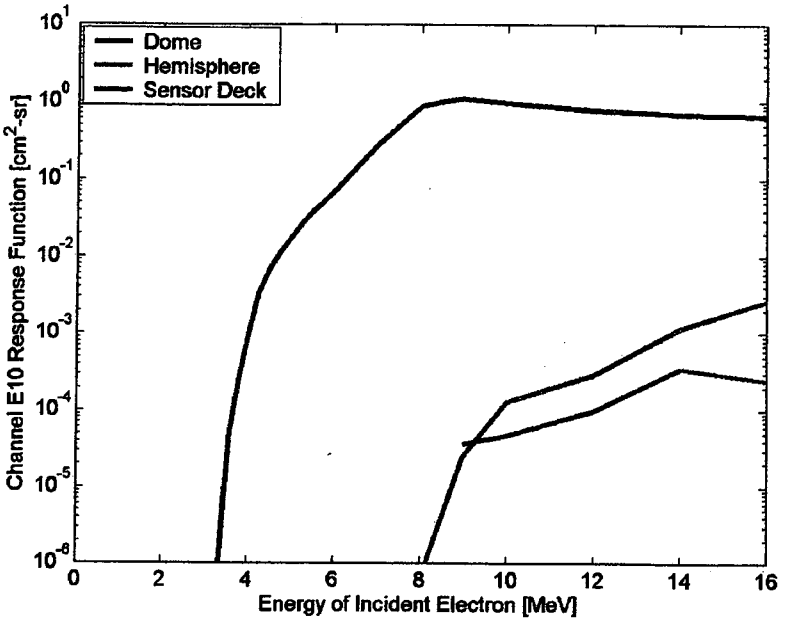

Figure 12. The same quantities as shown in Fig. 8, but for Channel E10.

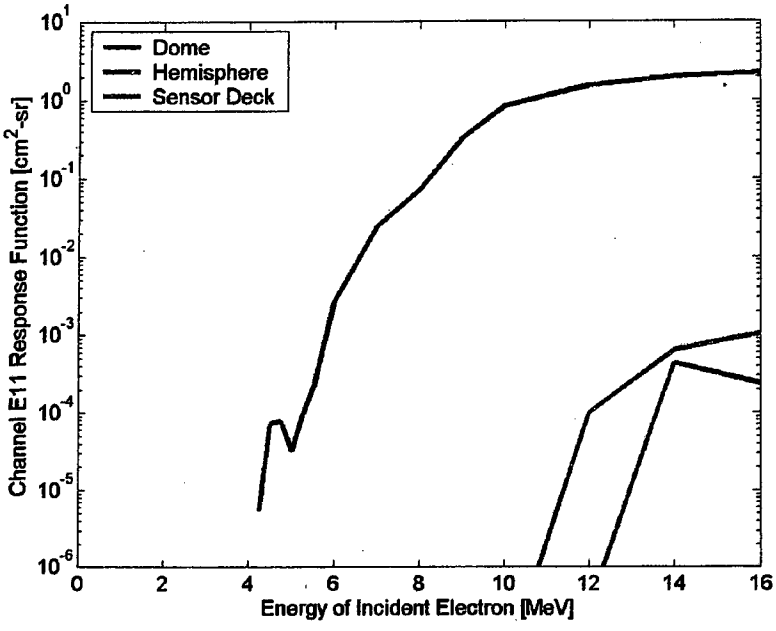

Figure 13. The same quantities as shown in Fig. 8, but for Channel E11.

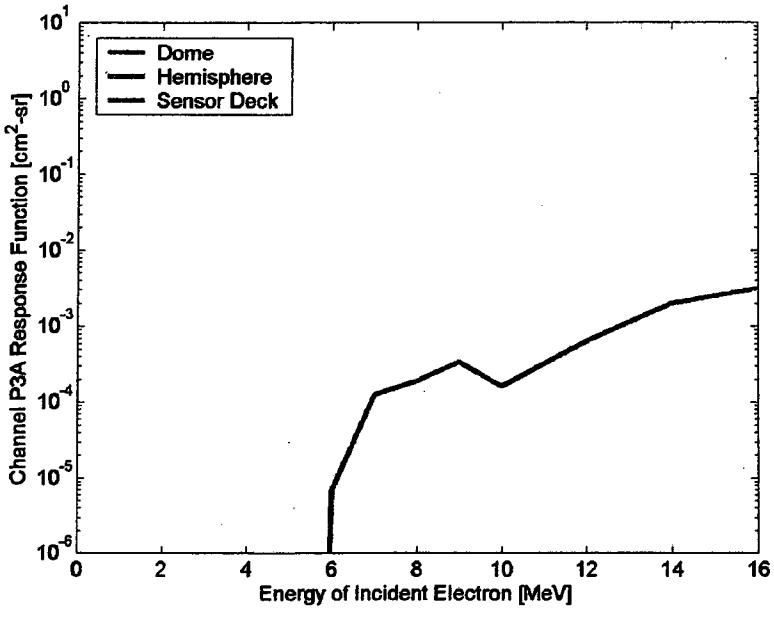

Figure 14. The same quantities as shown in Fig. 8, but for Channel P3A.

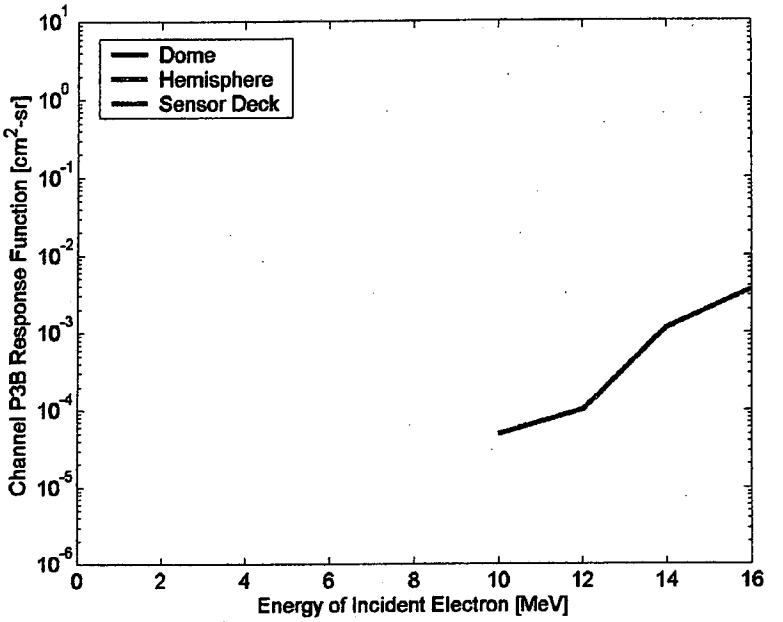

Figure 15. The same quantities as shown in Fig. 8, but for Channel P3B.

Appendix B: Proton Response Functions

(All 16 channels respond to incident protons)

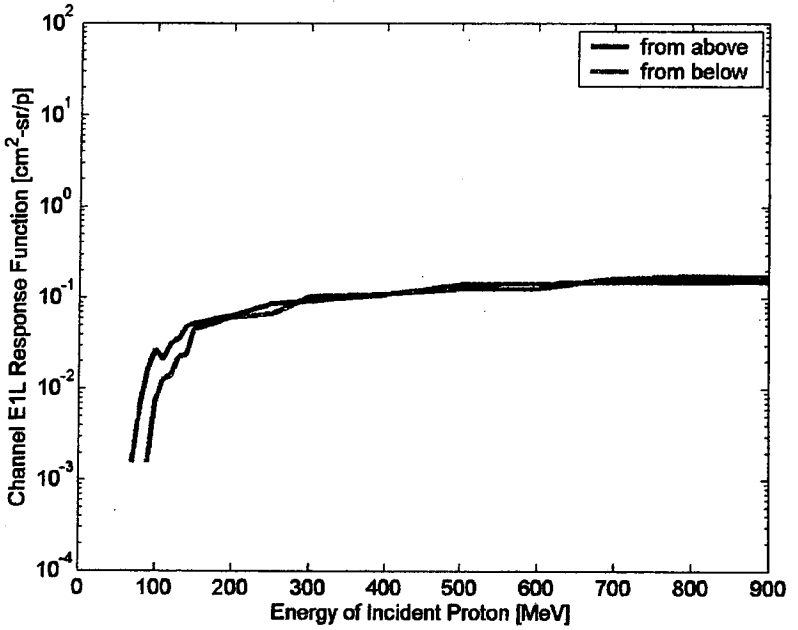

Figure 16. The numerically computed flux response of Channel E1L for an isotropic flux of protons incident on the LEP subassembly. The red line represents the response from protons incident on the LEP simulation geometry from above. The blue line, the response from protons incident on the simulation geometry from below.

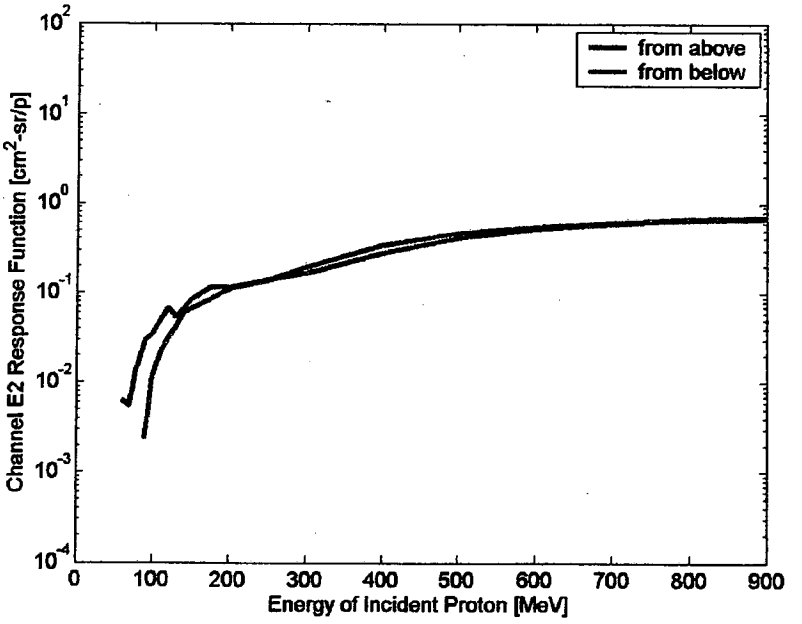

Figure 17. The same quantities as shown in Fig. 16, but for Channel E2.

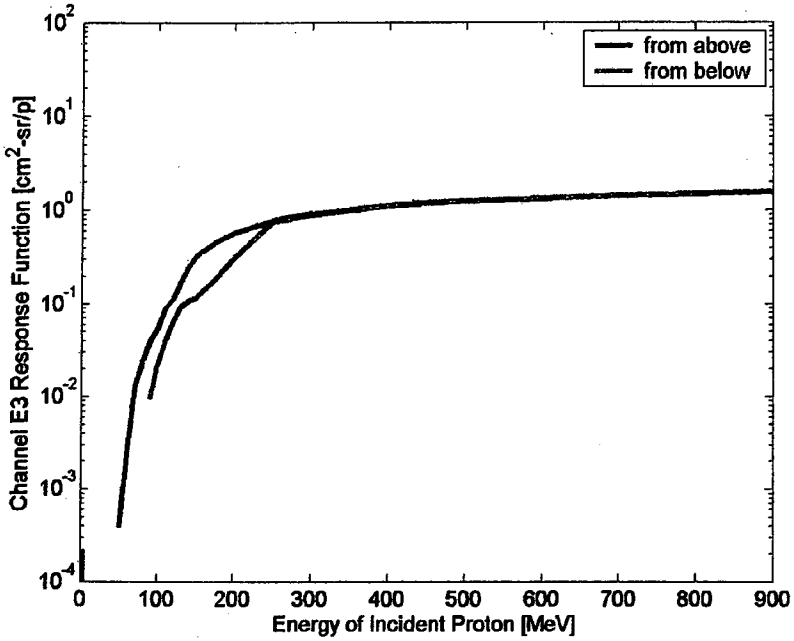

Figure 18. The same quantities as shown in Fig. 16, but for Channel E3.

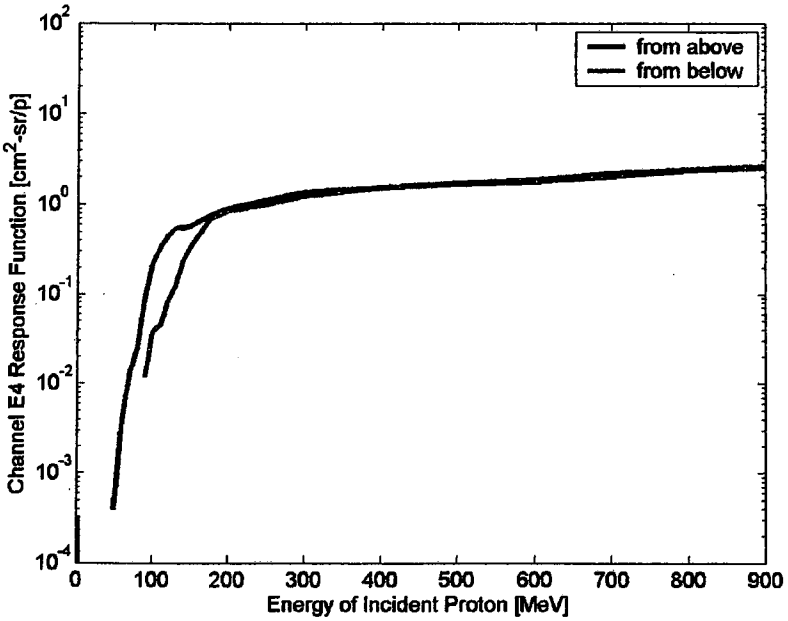

Figure 19. The same quantities as shown in Fig. 16, but for Channel E4.

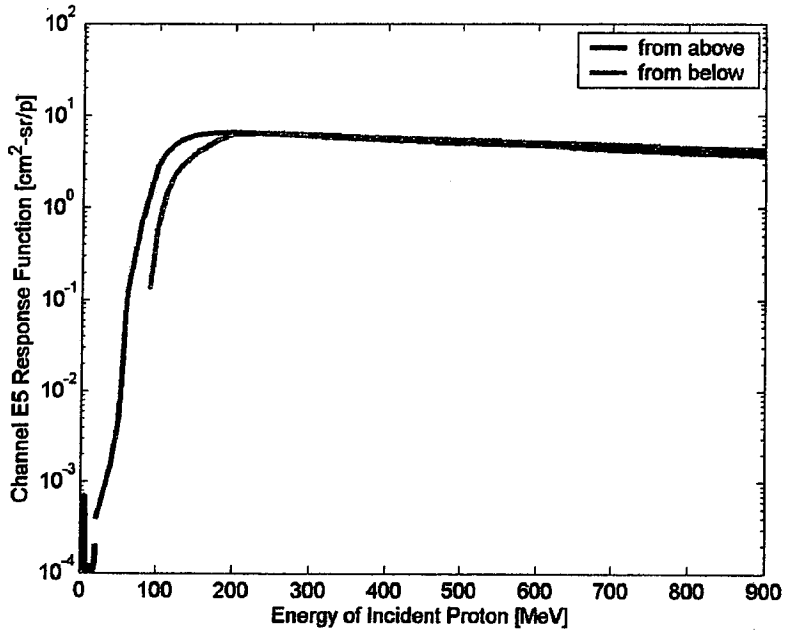

Figure 20. The same quantities as shown in Fig. 16, but for Channel E5.

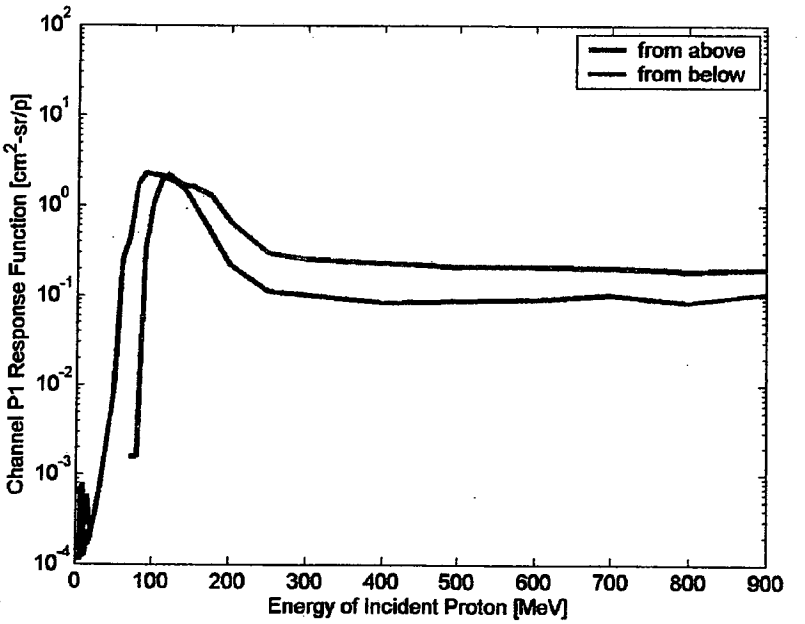

Figure 21. The same quantities as shown in Fig. 16, but for Channel P1.

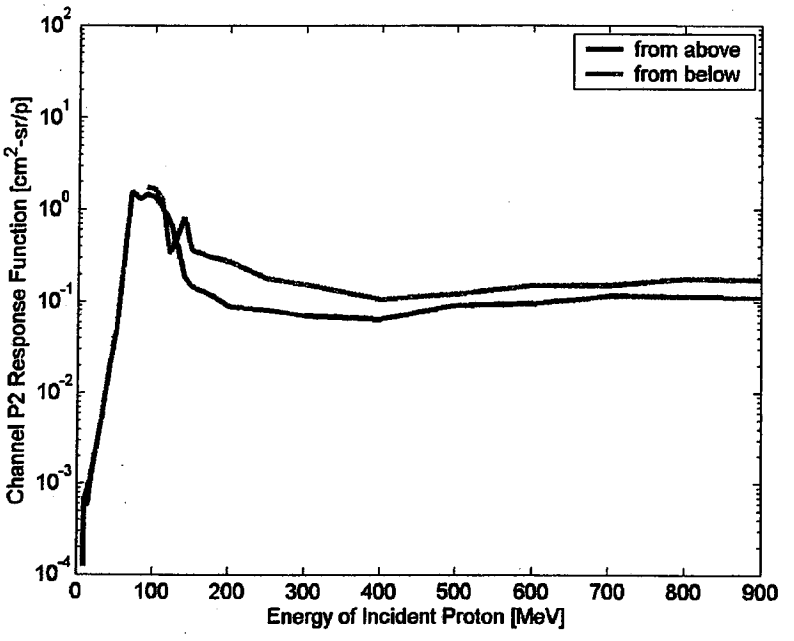

Figure 22. The same quantities as shown in Fig. 16, but for Channel P2.

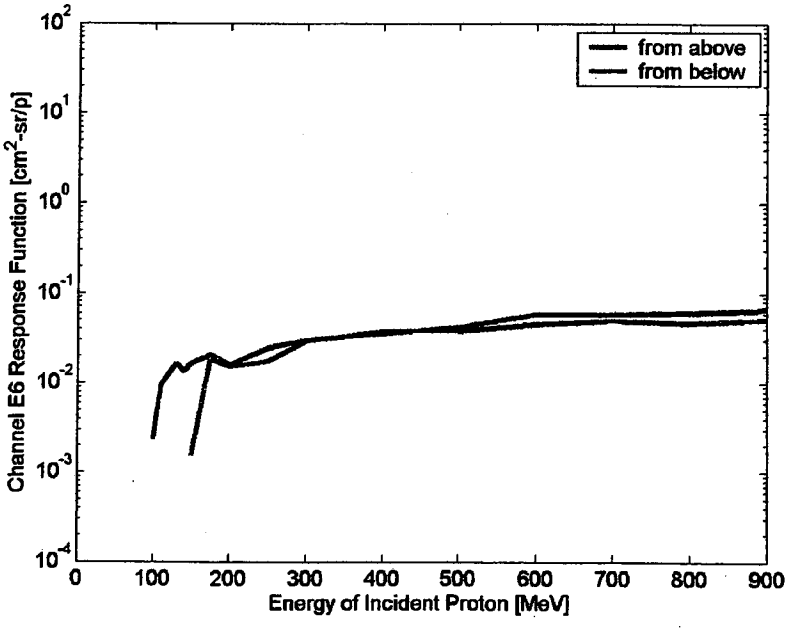

Figure 23. The numerically computed flux response of Channel E6 for an isotropic flux of protons incident on the HXP1 subassembly. The red line represents the response from protons incident on the HXP1 simulation geometry from above. The blue line, the response from protons incident on the simulation geometry from below.

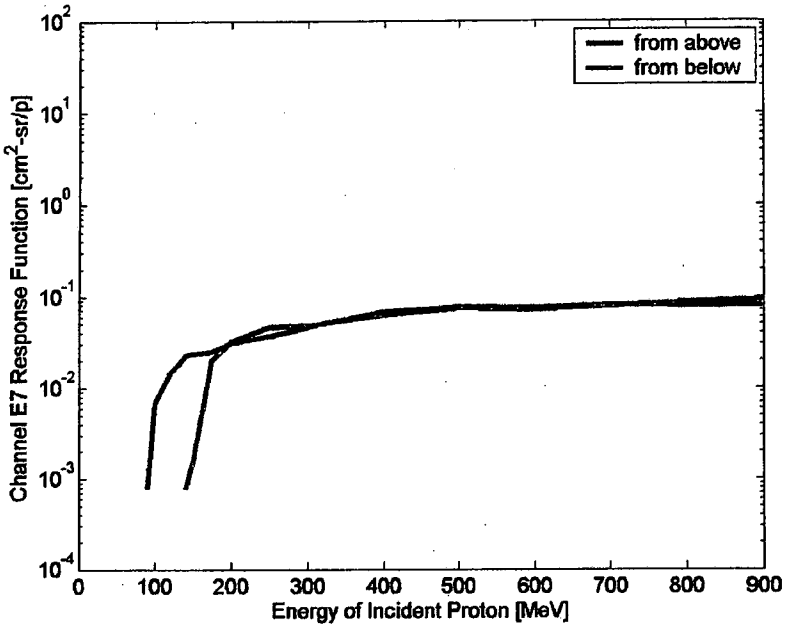

Figure 24. The same quantities as shown in Fig. 23, but for Channel E7.

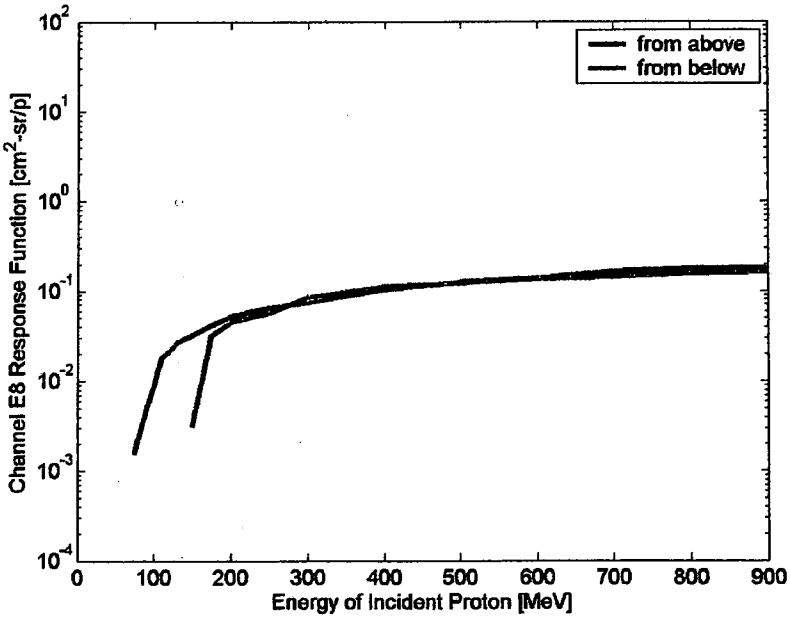

Figure 25. The same quantities as shown in Fig. 23, but for Channel E8.

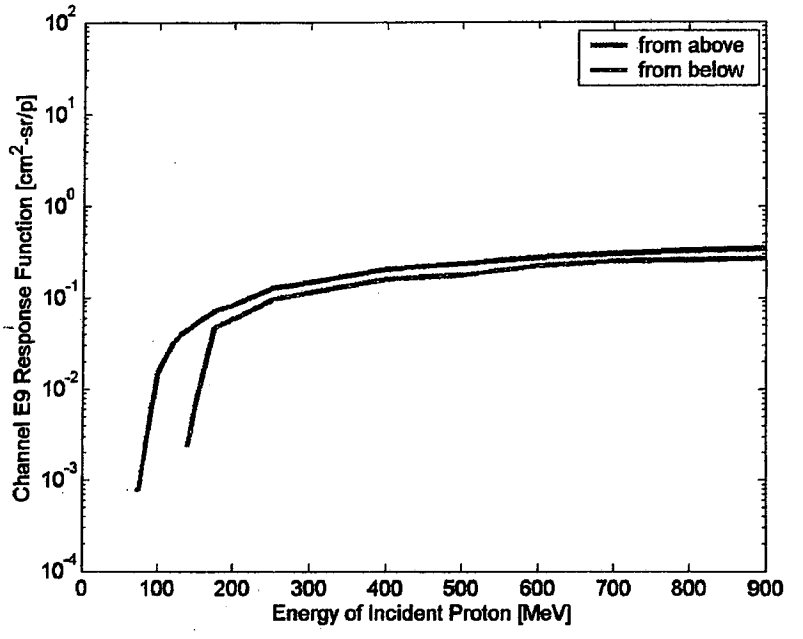

Figure 26. The same quantities as shown in Fig. 23, but for Channel E9.

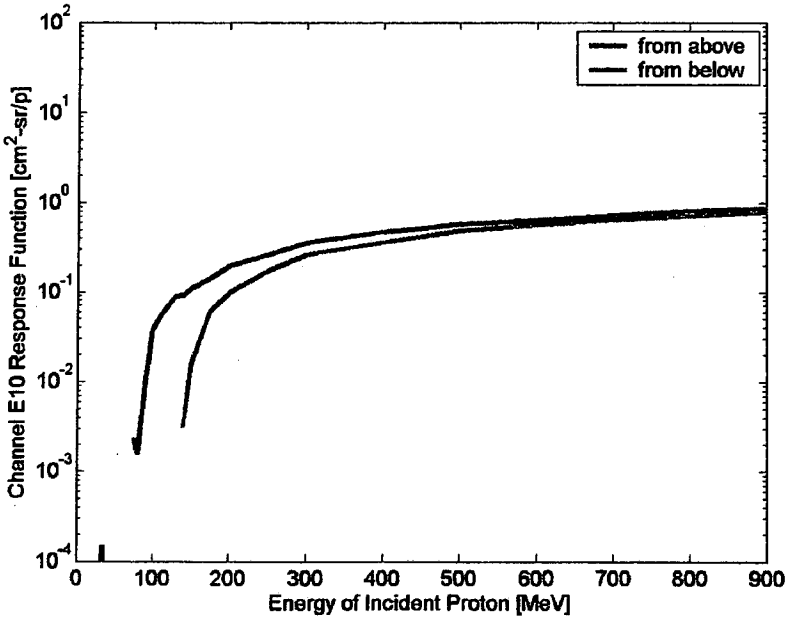

Figure 27. The same quantities as shown in Fig. 23, but for Channel E10.

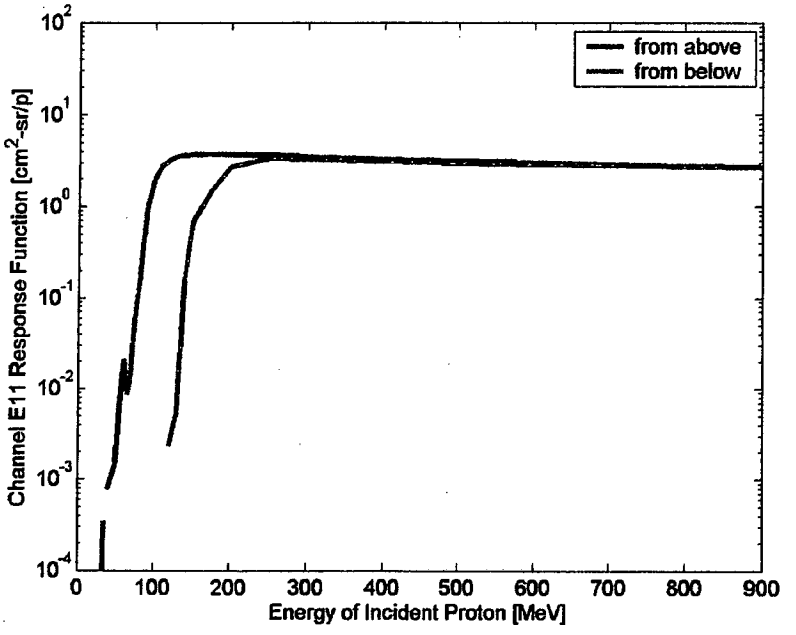

Figure 28. The same quantities as shown in Fig. 23, but for Channel E11.

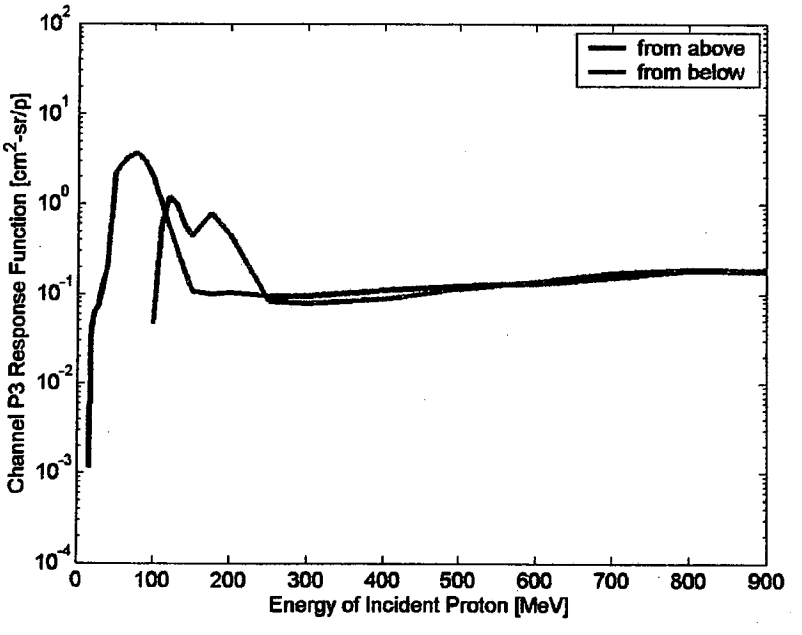

Figure 29. The same quantities as shown in Fig. 23, but for Channel P3.

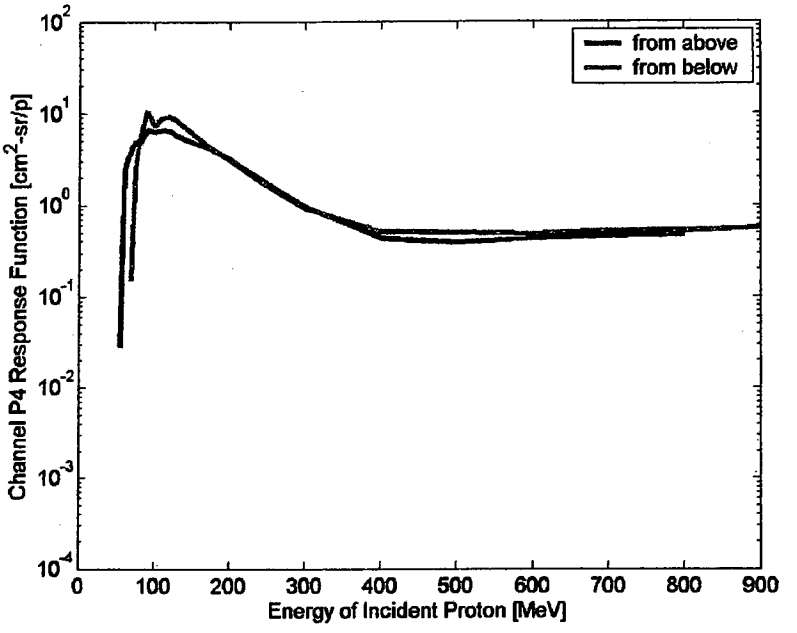

Figure 30. The numerically computed flux response of Channel P4 for an isotropic flux of protons incident on the HXP2 subassembly. The red line represents the response from protons incident on the HXP2 simulation geometry from above. The blue line, the response from protons incident on the simulation geometry from below.

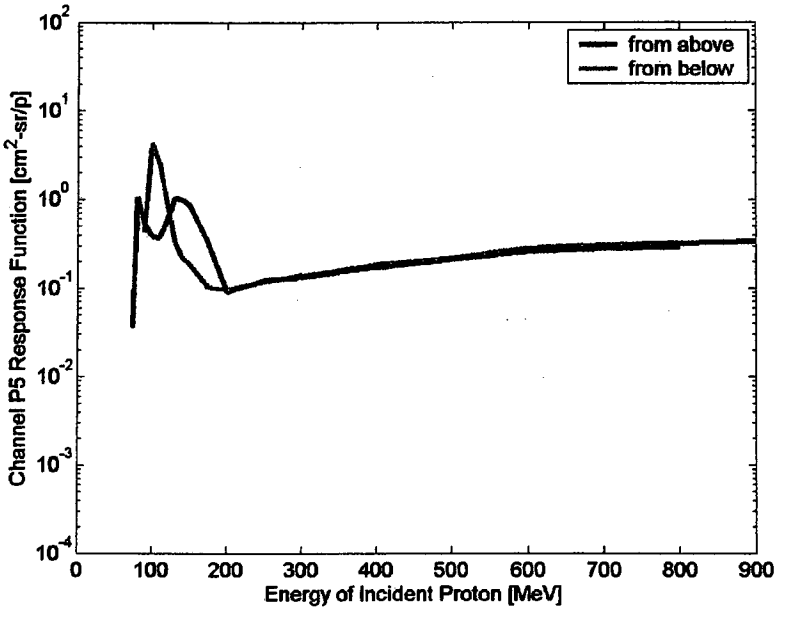

Figure 31. The same quantities as shown in Fig. 30, but for Channel P5.